THE JOURNAL OF BIOLOGICAL CHEMISTRY VOL. 287, NO. 29, pp. 24597–24603, July 13, 2012

Reconstitution of Vacuolar-type Rotary H^+-ATPase/Synthase from *Thermus thermophilus*[*] [S] [◆]

Received for publication, April 3, 2012, and in revised form, May 8, 2012 Published, JBC Papers in Press, May 11, 2012, DOI 10.1074/jbc.M112.367813

Jun-ichi Kishikawa and Ken Yokoyama[1]

From the Department of Molecular Biosciences, Kyoto Sangyo University, Kamigamo-Motoyama, Kita-ku, Kyoto 603-8555, Japan

Background: The V_oV_1 is composed of the hydrophilic V_1 and the membrane-embedded V_o.
Results: Intact V_oV_1 and shaftless complexes can be reconstituted from individual subunits *in vitro*.
Conclusion: The A_3B_3 domain tightly associates with the two EG peripheral stalks of V_o, even in the absence of the central shaft subunits.
Significance: The peripheral stalks are the major factor for the association of V_1 with V_o.

Vacuolar-type rotary H^+-ATPase/synthase (V_oV_1) from *Thermus thermophilus*, composed of nine subunits, A, B, D, F, C, E, G, I, and L, has been reconstituted from individually isolated V_1 ($A_3B_3D_1F_1$) and V_o ($C_1E_2G_2I_1L_{12}$) subcomplexes *in vitro*. A_3B_3D and A_3B_3 also reconstituted with V_o, resulting in a holoenzyme-like complexes. However, A_3B_3D-V_o and A_3B_3-V_o did not show ATP synthesis and dicyclohexylcarbodiimide-sensitive ATPase activity. The reconstitution process was monitored in real time by fluorescence resonance energy transfer (FRET) between an acceptor dye attached to subunit F or D in V_1 or A_3B_3D and a donor dye attached to subunit C in V_o. The estimated dissociation constants K_d for V_oV_1 and A_3B_3D-V_o were ~0.3 and ~1 nM at 25 °C, respectively. These results suggest that the A_3B_3 domain tightly associated with the two EG peripheral stalks of V_o, even in the absence of the central shaft subunits. In addition, F subunit is essential for coupling of ATP hydrolysis and proton translocation and has a key role in the stability of whole complex. However, the contribution of the F subunit to the association of A_3B_3 with V_o is much lower than that of the EG peripheral stalks.

Vacuolar-type ATPases (V_oV_1) are members of the rotary ATPase/ATP synthase superfamily, which catalyze the exchange between energy generated by proton translocation across a membrane and energy generated by ATP hydrolysis/synthesis (1–4). They are widely distributed in eukaryotic cells and bacteria (5, 6). Most prokaryotic V_oV_1 (also referred to as A-ATPase or A_oA_1 (1, 2)) produce ATP using the energy stored in a transmembrane electrochemical proton gradient (3, 7), whereas the V_oV_1 of some anaerobic bacteria, such as *Enterococcus hirae*, function as a sodium pump (8).

Thermus thermophilus V_oV_1 is capable of both ATP-driven proton translocation and proton-driven ATP synthesis *in vitro* and functions as an ATP synthase *in vivo* (3). The subunit structure of this V_oV_1 is simpler than the eukaryotic counterpart, being composed of nine subunits, A, B, D, F, C, E, G, I, and L. Each subunit shows a significant sequence similarity to its eukaryotic counterpart (supplemental Table 1). Several lines of evidence had previously suggested that the D, F, C, and L subunits form a central rotor with the I, E, and G subunits, constituting a stator apparatus together with the A_3B_3-hexamer (2, 9, 10) (Fig. 1). The recent cryo-EM map finally confirmed this subunit arrangement for *T. thermophilus* V_oV_1 (11).

The ATPase-active V_1 domain is composed of four subunits with a stoichiometry of $A_3B_3D_1F_1$ (12). The central rotor of V_1 is composed of two different subunits, D and F, with subunit F functioning as an activator of ATPase activity (13). In contrast, the equivalent subunit in F_1-ATPase, subunit ϵ, functions as an endogenous regulator of ATPase activity. However, the precise function of subunit F in the holoenzyme remains as yet unknown.

V_oV_1 and F-type ATPases (F_oF_1) are evolutionary related and share the rotary mechanism coupling ATP synthesis/hydrolysis and proton translocation across the membrane (1, 2). However, these two types of ATPase exhibit significant differences. The reversible association/dissociation of the catalytic and membrane-associated subcomplexes is unique to V_oV_1 and thought to be key for regulation of activity (14). Glucose deprivation has been shown to cause rapid dissociation of yeast V_oV_1 into free V_1 and V_o, a process that is both reversible and independent of *de novo* protein synthesis. For eukaryotic V_oV_1, two groups had reported reconstitution of V_oV_1 *in vitro* (15, 16). However, the dynamics of the reconstitution of V_oV_1 have not been reported.

In addition, significant differences are observed between the overall features of the two ATPases, particularly in the stalk region. The central stalk is considerably longer in V_oV_1 than in F_oF_1 (17). Subunit C (eukaryotic d subunit) is located at the interface between V_1 and the proteolipid ring, and this subunit is a major contributor to the extra length of the stalk region (18). This fact indicates the central shaft composed of subunits D and F does not contact the proteolipid ring directly. V_oV_1 also has a more complex peripheral stalk structure than F_oF_1. The stator structure of bacterial F_oF_1 consists of a single peripheral stalk formed by subunit b, whereas electron microscopic images of V_oV_1 suggest that V_1 is connected with V_o by two or

* This work was partly supported by Grants-in-aid from the Ministry of Education, Science, Sports and Culture of Japan (No. 21370042 and 24370059, to K. Y.) and TPRP (B-37, to K. Y.).
⌘ *Author's Choice*—Final version full access.
◆ This article was selected as a Paper of the Week.
[S] This article contains supplemental Table 1 and Fig. 1.
[1] To whom correspondence should be addressed. Tel.: 81-75-705-3043; Fax: 81-75-705-1914; E-mail: yokoken@cc.kyoto-su.ac.jp.

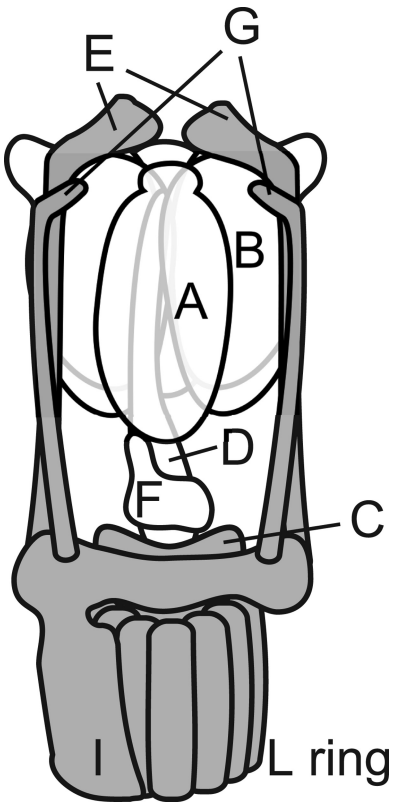

FIGURE 1. **Schematic representation of *T. thermophilus* V_oV_1.** Subunits in V_1 and in V_o are shown in *white* and *gray*, respectively.

three peripheral stalks (11, 17, 19). The complex structure of the V_oV_1 stalk seems to be relevant for a comparatively more rigid association of V_1 with V_o.

In this study, we show *in vitro* reconstitution of *T. thermophilus* V_oV_1 from isolated V_1 and V_o. The reconstitution in real time was measured by fluorescence resonance energy transfer (FRET) analysis using labeled V_1 and V_o, and thermodynamic parameters for the reconstitution were calculated. In addition, A_3B_3 and A_3B_3D subcomplexes also associated with V_o, suggesting that the peripheral stalks are mainly responsible for connecting V_1 to V_o.

EXPERIMENTAL PROCEDURES

Isolation of V_o—Wild-type or mutant V_oV_1 (C-S105C/C-C268S/C-C323S) *T. thermophilus* strains incorporating a His_8 tag on the N terminus of subunit A were generated by the integration vector system (20). The modified *T. thermophilus* strains were cultured as described previously (9). The cells (200 g) harvested at log phase growth were suspended in 400 ml of 50 mM Tris-Cl (pH 8.0), containing 5 mM $MgCl_2$, and disrupted by sonication. The membranes were precipitated by centrifugation at 100,000 × *g* for 20 min and washed with the same buffer twice. The washed membranes were suspended in 20 mM imidazole sodium (pH 8.0), 0.1 M NaCl, and 10% Triton X-100 (w/v), and the suspension was sonicated. Cell debris and insoluble material were removed by centrifugation at 100,000 × *g* for 60 min, and the supernatant was applied onto a nickel-nitrilotriacetic acid superflow column (Qiagen, 3 × 5 cm) equilibrated with 20 mM imidazole sodium (pH 8.0), 0.1 M NaCl, 0.1% Triton X-100. The column was washed with 200 ml of the same buffer. The protein was eluted with a linear imidazole gradient (20–100 mM). The fractions containing the V_oV_1 were applied to a RESOURCE Q column (6 ml, GE healthcare) equilibrated with 20 mM Tris-Cl (pH 8.0), 0.1 mM EDTA, and 0.05% *n*-dodecyl-β-D-maltoside (Sigma). The proteins were eluted with a linear NaCl gradient (0–0.5 M). Each fraction containing V_o was combined and concentrated and then subjected to FPLC with a Superdex HR-200 column (GE healthcare) equilibrated with MOPDM buffer (20 mM MOPS, pH 7.0, 100 mM NaCl, 0.05% *n*-dodecyl-β-D-maltoside). The proteins were eluted with the same buffer. The mutated V_o (C-S105C/C-C268S/C-C323S) was used for the FRET experiments. The V_o fractions were combined and used immediately.

Isolation of V_1 (A_3B_3DF), A_3B_3D, and A_3B_3—Escherichia coli strain BL21-CodonPlus-RP (Stratagene) was used for expression of V_1 (A_3B_3DF), A_3B_3D, and A_3B_3. These recombinant subcomplexes were isolated as described previously (13). The expressed cells were suspended in 20 mM imidazole/HCl (pH 8.0) containing 0.3 M NaCl and disrupted by sonication. After removal of heat labile proteins derived from the host cells by heat treatment at 65 °C for 30 min, the solution was applied to an Ni^{2+} affinity column (Qiagen, 3 × 5 cm), which was then washed thoroughly and eluted with 0.5 M imidazole/HCl (pH 8.0) containing 0.3 M NaCl. The buffer was exchanged to 20 mM Tris/HCl (pH 8.0) containing 1 mM EDTA by ultrafiltration (Vivaspin, Vivascience), and the solution was applied to a RESOURCE Q column. The fractions containing subcomplexes were concentrated, and contaminating proteins were removed on a Superdex HR-200 column equilibrated with MOPDM buffer. The mutant V_1 (A-His_8/ΔCys, A-C255A/A-S232A/A-T235S/F-S54C), mutant A_3B_3 (A-His_8/ΔCys, A-C255A/A-S232A/A-T235S), and mutant A_3B_3D (A-His_8/ΔCys, A-C255A/A-S232A/A-T235S, A-His_8/ΔCys, A-C255A/A-S232A/A-T235S, D/E48C) were used for either reconstitution or FRET experiments.

Reconstitution of V_oV_1, A_3B_3D-V_o, and A_3B_3-V_o—The purity of each subcomplex was confirmed by SDS- and AES-PAGE,[2] a nondenaturing PAGE suitable for analysis of membrane protein complexes. V_1, A_3B_3D, or A_3B_3 (each >1 mg/ml) in MOPDM buffer was mixed with 1 mg/ml V_o solution at an equal volume ratio. For reconstitution of V_oV_1, a range of different concentrations of V_o was added into V_1 solution, and then the mixtures were incubated at 25 °C for 1 h. The mixtures were incubated for 1 h at 25 °C and then applied onto the Superdex HR-200 column equilibrated with the same buffer. The reconstituted complexes were collected and used for further analysis immediately.

FRET Analysis—The purified V_1 (A-His_8/ΔCys, A-C255A/A-S232A/A-T235S/F-S54C) or A_3B_3D (A-His_8/ΔCys, A-C255A/A-S232A/A-T235S, D/E48C) was immediately labeled with a 2 M excess of Cy3™-maleimide (GE healthcare, used as a donor molecule) in MOPDM buffer. Following a 60-min incubation at 25 °C, proteins were separated from unbound reagent with a PD-10 column (GE Healthcare). The mutated V_o

[2] The abbreviations used are: AES-PAGE, alkyl ether sulfate-PAGE; DCCD, dicyclohexylcarbodiimide.

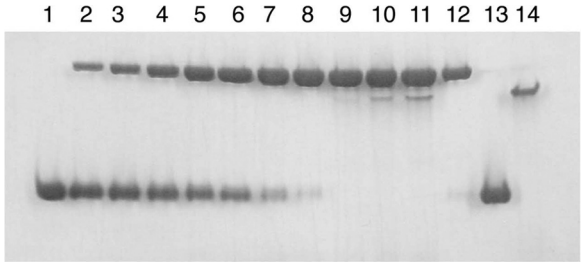

FIGURE 2. **AES-PAGE analysis of V_oV_1 reconstituted from the individually isolated V_1 and V_o subcomplexes.** Reconstitution was performed by the addition of 20 μl of MOPDM buffer containing increasing amounts of V_o into 20 μl of 2 μM V_1 solution. Following incubation, half of each test condition was loaded onto the gel. Proteins were stained by Coomassie Brilliant Blue. The amount of added V_o was, 0, 2, 4, 6, 8, 10, 12, 14, 16, 18, and 20 μg (*lanes 1–11*). *Lane 12*, V_oV_1 from *T. thermophilus*; *lane 13*, V_1; *lane 14*, V_o. The *lower band* corresponds to free V_1, and the *upper band* corresponds to the V_oV_1 complex.

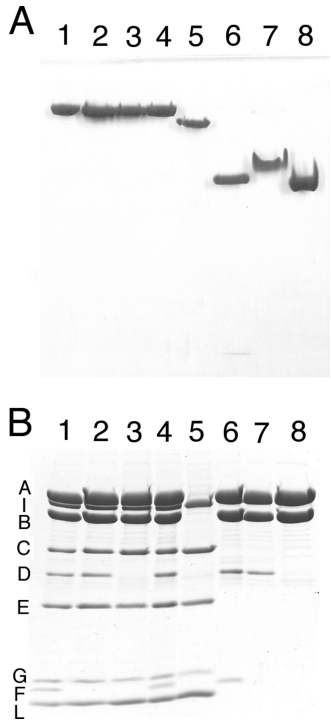

FIGURE 3. **AES- and SDS-PAGE analysis of the reconstituted complexes.** *A* and *B*, the isolated reconstituted complexes were subjected to AES (*A*) or SDS-PAGE (*B*). The proteins were stained by Coomassie Brilliant Blue. *Lane 1*, the reconstituted V_oV_1; *lane 2*, the reconstituted A_3B_3D-V_o; *lane 3*, the reconstituted A_3B_3-V_o; *lane 4*, the V_oV_1 from *T. thermophilus*; *lane 5*, the V_o from *T. thermophilus*; *lane 6*, V_1 (A_3B_3DF); *lane 7*, A_3B_3D; *lane 8*, A_3B_3.

(C-S105C/C-C268S/C-C323S) was labeled with Cy5™-maleimide (GE Healthcare, used as an acceptor molecule) by the same method described above. The specific labeling of subunit F in V_1 or subunit C in V_o was checked by measurement of each subunit fluorescence. FRET signals as a result of reconstitution of V_oV_1 were monitored with a fluorometer using an excitation wavelength of 532 nm and an emission wavelength of 570 nm (FP-3000, Hitachi). Typically, a quartz cuvette was filled with 1.2 ml of MOPDM buffer containing 5 nM labeled V_1 or A_3B_3D and incubated at 25 °C until the fluorescence intensity reached a constant level. For measurement of binding kinetics, 10 μl of V_o-C105C-Cy5 at the indicated final concentration was added into the cuvette.

Other Assays—Protein concentrations of V_1 were determined from UV absorbance calibrated by quantitative amino acid analysis; 1 mg/ml gives an optical density of 0.88 at 280 nm. Protein concentrations of V_o and V_oV_1 were determined by BCA protein assay, and V_1 was used as protein standard. ATPase activity was measured at 25 °C with an enzyme-coupled ATP regenerating system. The ATPase assay solution contained 50 mM Tris-HCl (pH 8.0), 100 mM KCl, 2 mM $MgCl_2$, 4 mM Mg-ATP, 2 mM phosphoenolpyruvate, 100 μg/ml lactate dehydrogenase, 100 μg/ml pyruvate kinase, 0.2 mM NADH, and 0.05% *n*-dodecyl-β-D-maltoside. Polyacrylamide gel electrophoresis in the presence of SDS or AES was carried out as described previously (9). The proteins were stained with Coomassie Brilliant Blue. For measurement of ATP synthesis activity, the ATPases were reconstituted into liposome with bacteriorhodopsin, and light-induced ATP synthesis activities were measured as described previously (21).

RESULTS

Reconstitution of V_oV_1 from Isolated V_o and V_1—The V_o and V_1 of *T. thermophilus* were isolated from membranes of *T. thermophilus* expressing His_8-tagged V_oV_1 and further purified by gel permeation column chromatography. SDS-PAGE and AES-PAGE confirmed the purity of the subcomplexes (Figs. 2 and 3). Reconstitution of V_oV_1 was confirmed with AES-PAGE (Figs. 2 and 3*A*). With increasing concentrations of V_o, there is a steady decrease in the levels of free V_1 and a concomitant increase in the levels of V_oV_1. At a concentration of 16 μg or above of V_o, all the V_1 is reconstituted into V_oV_1 (Fig. 2). This result clearly indicates that the isolated V_o and V_1 assemble into V_oV_1 with a very low dissociation constant (K_d).

Reconstitution of A_3B_3D-V_o and A_3B_3-V_o Complex—The ability of the A_3B_3D and A_3B_3 subcomplexes to reconstitute with V_o was also assessed to determine whether the central stalk is necessary for reconstitution. The purity and subunit stoichiometry of the A_3B_3D and A_3B_3 subcomplexes were confirmed by SDS-PAGE and AES-PAGE (Fig. 3, *A* and *B*, *lanes 7* and *8*). When an excess of A_3B_3D was incubated with V_o, a new gel permeation peak was observed with the same retention time as V_oV_1 (data not shown). SDS-PAGE analysis revealed that the peak was composed of subunits A, B, C, D, I, E, G, and L (Fig. 3*B*). The A_3B_3D-V_o reconstituted complex migrated as a single band on AES-PAGE with the same mobility as V_oV_1. Gel permeation HPLC and AES-PAGE (Fig. 3) also showed that the A_3B_3 was also able to form a stable complex with V_o. SDS-PAGE analysis confirmed that the complex did not include the D and F subunits (Fig. 3*B*). The results clearly indicate that the central shaft subunits D and F are not essential for reconstitution of a stable complex between the A_3B_3 domain and V_o.

Properties of the Reconstituted Complexes—Both the ATP hydrolysis and the synthesis activity of the reconstituted complexes were investigated. The reconstituted V_oV_1 exhibited simple Michaelis-Menten kinetics with a K_m value of 420 ± 80 μM and a k_{cat} of about 16 ± 2.0 s^{-1}. These values are in the same range as those obtained for the wild-type enzyme (3). Fig. 4*A* shows the sensitivity of the reconstituted complex to inactivation by DCCD, a specific inhibitor that modifies a critical carboxylate in the proteolipid subunit. An ability to be inhibited by

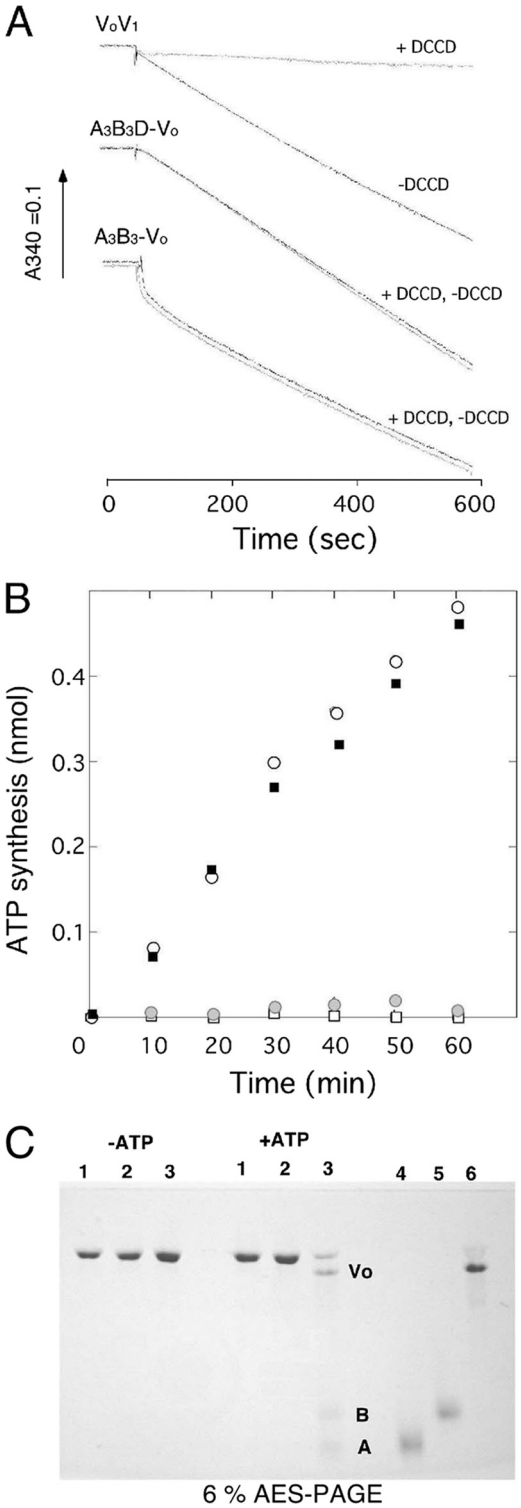

FIGURE 4. **Enzymatic properties of the reconstituted complexes.** *A*, DCCD sensitivity of the reconstituted complexes. Each reconstituted complex was incubated with 50 μM DCCD for 30 min in MOPDM buffer, and ATPase activity was measured as described under "Experimental Procedures." In control experiments, the reconstituted complexes were treated in the same way with the exception that DCCD was not included. *B*, ATP synthesis activity of the reconstituted complexes in proteoliposomes. *Open circles*, V_oV_1; *closed squares*, the reconstituted V_oV_1; *open squares*, the A_3B_3D-V_o; *gray circles*, the A_3B_3-V_o. *C*, effect of ATP on the reconstituted complexes. The reconstituted complexes were incubated for 1 h at 25 °C in the absence (*left*) or presence (*right*) of 2 mM ATP, submitted to AES-PAGE analysis. *Lane 1*, the V_oV_1; *lane 2*, A_3B_3D-V_o; *lane 3*, A_3B_3-V_o; *lane 4*, A subunit; *lane 5*, B subunit; *lane 6*, V_o.

DCCD is an indication that an F_oF_1 complex is intact; if proton translocation and ATP hydrolysis are uncoupled due to damage of the functional connection between F_o and F_1, ATPase activity is no longer sensitive to DCCD inhibition (22). The ATPase activity of reconstituted V_oV_1 was inhibited by DCCD and almost completely lost 30 min after the addition of the inhibitor (Fig. 4*A*). The reconstituted V_oV_1 was also capable of ATP synthesis activity; vesicles containing bacteriorhodopsin and the V_oV_1 synthesized ATP following illumination. The ATP synthesis activity of reconstituted V_oV_1 was comparable with that of wild V_oV_1 (Fig. 4*B*). These results indicate that the reconstituted V_oV_1 is functional.

The turnover rate of A_3B_3D-V_o was ~20 s^{-1} at the same range of activity of the A_3B_3D complex reported previously (13). ATP hydrolysis by A_3B_3-V_o proceeded in two distinct phases: an initial rapid phase and a slow steady state phase (~10 s^{-1}, Fig. 4*A*). In contrast to the V_1 complex, the A_3B_3 subcomplex showed an initial rapid phase, and ATPase activity was gradually lost due to ATP-induced disassembly of the A_3B_3 subcomplex (23). The ATP hydrolysis profile of A_3B_3-V_o was mostly identical to that of the A_3B_3 subcomplex, suggesting that the association of V_o and A_3B_3 does not change the catalytic properties of A_3B_3 domain and that A_3B_3-V_o gradually disassembles during ATP hydrolysis. In fact, both reconstituted V_oV_1 and reconstituted A_3B_3D-V_o were resistant to the ATP-induced disassembly; however, the reconstituted A_3B_3-V_o disassembled into V_o and monomeric A and B subunits following the addition of ATP (Fig. 4*C*). This result indicates that the association of V_o and A_3B_3 does not prevent ATP-induced disassembly of the A_3B_3. Unlike the reconstituted V_oV_1, both the A_3B_3D-V_o and the A_3B_3-V_o did not show sensitivity to DCCD (Fig. 3*A*). In addition, no ATP synthesis activity was detected by reconstituted proteoliposome containing either A_3B_3D-V_o or A_3B_3-V_o (Fig. 4*B*). These results clearly indicate that the F subunit is essential for coupling ATP synthesis with proton translocation across the membrane.

Real-time Monitoring of Reconstitution by FRET—FRET is an excellent method for detecting protein association (24). To measure the reconstitution of V_oV_1 or A_3B_3D-V_o in real time, V_1, A_3B_3D, and V_o were labeled with different fluorescent dyes. The subunit F in V_1 (F-S54C) and the subunit D in A_3B_3D (D-E48C) were labeled with the maleimide derivative Cy3. For labeling of the subunit C in V_o, a cysteine was introduced at position 105, which was then labeled with Cy5 maleimide. The degree of labeling was ~80% for V_1, ~95% for A_3B_3D, and 80% for V_o as determined by UV-visible spectroscopy of the labeled complexes. The specificity of each labeling was confirmed by SDS-PAGE (supplemental Fig. 1). Reconstitutions were carried out in a quartz cuvette containing 1.2 ml of the V_1-F54C-Cy3 solution. Upon the addition of V_o-C105C-Cy5 to the V_1-F54C-Cy3, the emission intensity at 570 nm decreased, and an alternative peak at 650 nm was detectable (Fig. 5*A*). The magnitude of the peak at 650 nm initially depended on the amount of the added V_o-C105C-Cy5. Fluorescence at 570 nm decreased sharply upon the addition of the V_o-C105C-Cy5 (Fig. 5*B*). In comparison, the addition of excess nonlabeled V_o into V_1-F54C-Cy3 resulted in no decrease in fluorescence at 570 nm. These results clearly indicate that the decrease in fluores-

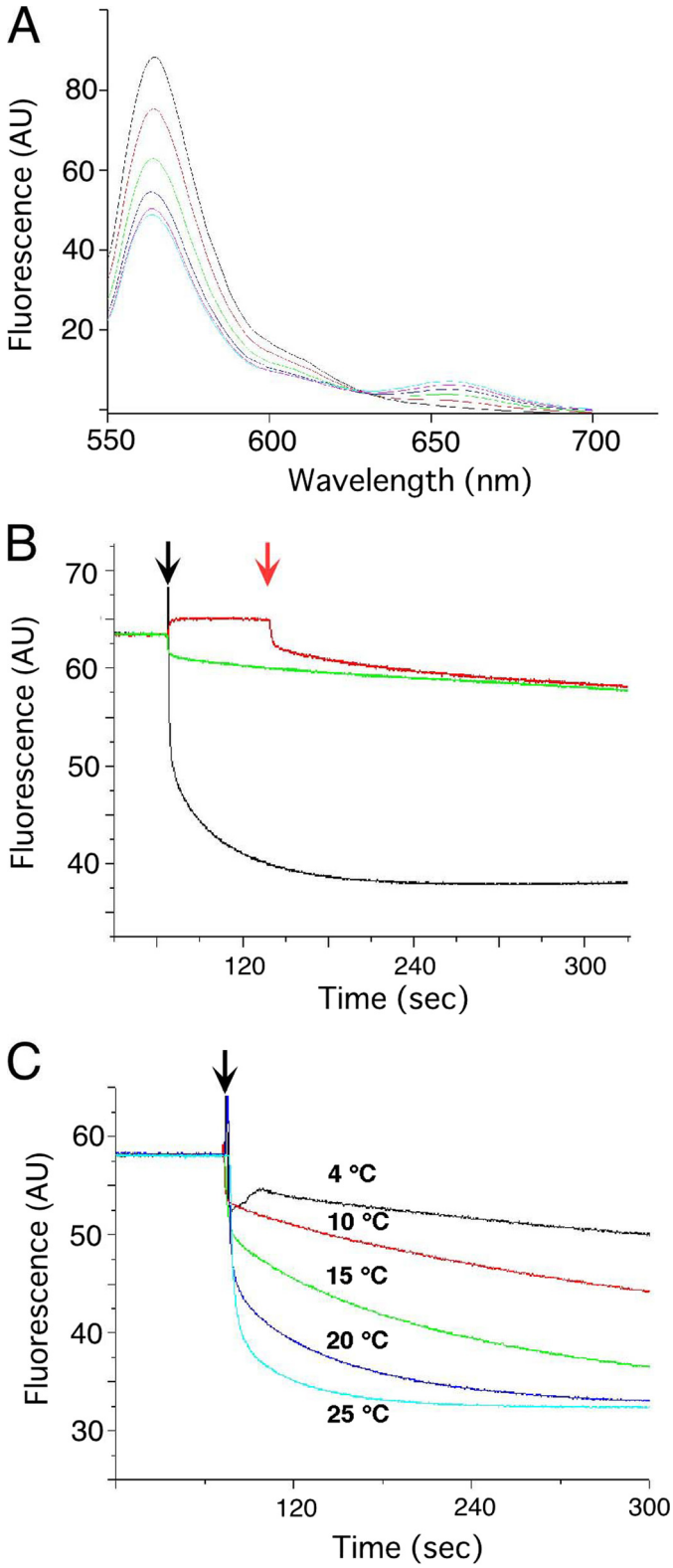

FIGURE 5. **Probing reconstitution of V_oV_1 by FRET.** *A*, fluorescence spectra of the donor at different concentrations of acceptor. Fluorescence spectra of V_1-F54C-Cy3 were recorded (final concentration of 23 nM, excitation at 532 nm). Different concentrations of V_o-C105C-Cy5 (0, 5, 10, 15, 20, 25 nM final concentration) were added. The test samples were incubated for 10 min, and then the fluorescence spectra of each mixture were measured. *A. U.*, arbitrary units. *B*, time course of the donor fluorescence. The *black line* shows the fluorescence obtained when 10 μl of 4 μM of V_o-C105C-Cy5 was added into a cuvette containing 23 nM V_1-F54C-Cy3 at the time indicated by the *black arrow*. The *red line* shows the fluorescence obtained when 10 μl of 5 μM V_o was added into a cuvette containing 23 nM V_1-F54C-Cy3 at the time indicated by the *black arrow*, and then a further 10 μl of 4 μM of V_o-C105C-Cy5 was added at the time indicated by the *red arrow*. The *green line* shows the fluorescence obtained when 10 μl of MOPDM buffer was added at the time indicated by the *black arrow*. *C*, temperature effect on the time course of donor fluorescence. 10 μl of 4 μM of V_o-C105C-Cy5 was added into a cuvette containing 23 nM V_1-F54C-Cy3 at the indicated temperature.

cence following the addition of V_o-C105C-Cy5 is due to reconstitution of V_oV_1. The rate of decrease in fluorescence at 570 nm and the associated increase in fluorescence at 650 nm following the addition of the acceptor is higher at 25 °C than at lower temperatures. Indeed there was no detectable decrease in fluorescence at 570 nm observed at 4 °C (Fig. 5*C*, *black line*). These results indicate that the association of V_1 and V_o is temperature-dependent.

To estimate the dissociation constant, K_d, for V_oV_1 into V_1 and V_o, a range of concentrations of V_o-C105C-Cy5 (0.1–1.2 nM final concentration) was modified to a single concentration of V_1-F54C-Cy3. The fluorescence intensity at 570 nm decreased with increasing concentration of V_o-C105C-Cy5 (Fig. 6*A*). The time-dependent changes were analyzed using a simple sequential model for the dissociation and association of the complexes, and the apparent rate constants were calculated by nonlinear regression fitting (25, 26) and plotted against the concentration of added V_o-C105C-Cy5 (Fig. 6*C*). The K_d was estimated to be 0.26 ± 0.23 nM ($n = 7$). The fluorescence of Cy3 in A_3B_3D-D48C-Cy3 was also decreased by the addition of V_o-C105C-Cy5 (Fig. 6*B*). The dissociation constant for the A_3B_3D-V_o was estimated to be 1.1 ± 0.54 nM ($n = 4$). The results suggest that the F subunit is not essential for association of A_3B_3 domain to V_o, but contributes to the stability of the complex.

DISCUSSION

In this study, we demonstrated the reconstitution of V_oV_1 of *T. thermophilus in vitro* by mixing individually isolated V_o and V_1 subcomplexes. The reconstitution was complete at equimolar concentrations of V_1 and V_o, indicating that both the isolated V_1 and the isolated V_o retain full reconstitution ability. The dissociation/association of V_oV_1 in prokaryotic cells has not been reported yet; however, our results suggest that the prokaryotic V_oV_1 is assembled by association of a cytosolic V_1 with a membrane-embedded V_o *in vivo*. In addition, we have demonstrated real-time reconstitution of V_oV_1 by FRET. The K_d for V_oV_1 is estimated as ~0.3 nM at 25 °C, giving a Gibbs free energy ($\Delta G°$) of binding of V_1 to V_o as ~54 kJ/mol with $\Delta G° = -RT\ln K_d$. Because the rate of reconstitution increases at higher temperature (Fig. 5*C*), a much lower K_d is predicted for V_oV_1 in *T. thermophilus* cells, whose optimum growth temperature is 60–80 °C. The low K_d indicates that the equilibrium between association/dissociation of V_oV_1 might be biased toward association of V_1 and V_o in the cells.

Surprisingly, A_3B_3D and A_3B_3 also associated with V_o, producing a holoenzyme-like complex lacking the F subunit or the central shaft DF subcomplex, respectively. Electron microscopic studies of V_oV_1 have indicated that the V_1 domain was connected to the V_o domain with two (11) or three peripheral stalks (27), whereas the stator structure of bacterial F_oF_1 con-

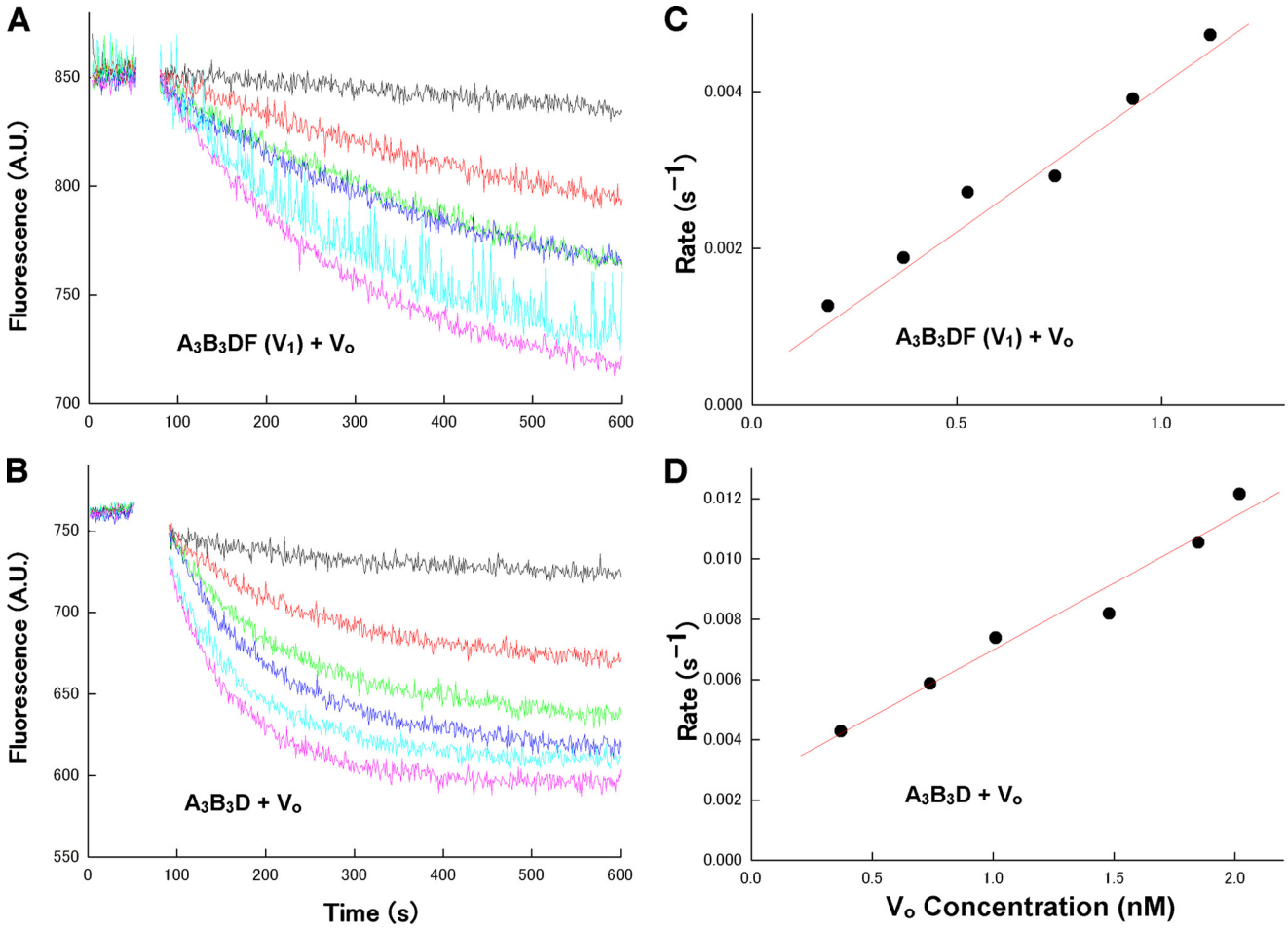

FIGURE 6. **Typical time course of donor fluorescence in presence of V_1 or A_3B_3D.** *A* and *B*, different concentrations of V_o-C105C-Cy5 as indicated in *panels C* and *D* were added into a cuvette with 1.2 ml of MOPDM buffer containing 80 pM V_1-F54C-Cy3 (*A*) or 130 pM A_3B_3D-D48C-Cy3 (*B*), and fluorescence changes of the donor were measured. *A. U.*, arbitrary units. *C* and *D*, apparent rate constants ($k^{app} = k_{on}$[ATP] $- k_{off}$) were determined by fitting the fluorescence decrease after the addition of V_o-C105C-Cy5 for V_1-F54C-Cy3 (*C*) or A_3B_3D-D48C-Cy3 (*D*) with a single exponential equation (25, 26), plotted against ATP concentrations ([ATP]). From a linear fit to the plot, k_{on} and k_{off} were calculated as a slope and an intercept, respectively (25).

sists of a single peripheral stalk formed by the b subunit (28). The results presented in this study suggest that the A_3B_3 domain is tightly associated with the two EG peripheral stalks of V_o, even in the absence of the central shaft subunits. The crystal structure of the F_1c_{10} of yeast (PDB ID: 3ZRY) indicated that the $\alpha_3\beta_3$ domain binds tightly to the proteolipid ring through the central shaft subunit γ and ϵ (29). In contrast, *T. thermophilus* V_oV_1 has a subunit C located in the central stalk, which caps one end of the subunit-L ring with the internal cavity of subunit C open toward the V_1 side to accommodate the shaft composed of the D and F subunits (18). The socket-like structure of the C subunit seems to be favorable for the reversible dissociation/association of the central shaft, but unfavorable for tight binding of the V_1 central shaft with V_o. It is likely that the instability of the V_oV_1 holoenzyme due to the detachable central stalk might be compensated for by the binding of the two EG peripheral stalks to V_1.

The reconstituted complex without subunit F hydrolyzed ATP, but did not show ATP synthesis activity or DCCD-sensitive ATPase activity. This indicates that ATP synthesis and proton translocation in the A_3B_3D-V_o were uncoupled due to complete loss of the functional connection between A_3B_3D and V_o. That is, *intramolecular uncoupling* of A_3B_3D-V_o should have occurred. In this case, the binding energy of the D subunit to the C subunit in the central stalk is thought to be much lower than the observed $\Delta G°$ for ATP synthesis, ~40 kJ/mol at 25 °C (30). The estimated K_d for A_3B_3D-V_o is ~1 nM, giving a $\Delta G°$ of binding of A_3B_3D to V_o as ~50 kJ/mol, slightly lower than that of V_oV_1 (~54 kJ/mol). This suggests that the F subunit reinforces the stability of whole complex, but the contribution of the F subunit to association of A_3B_3DF (V_1) with V_o is lower than that of two EG peripheral stalks.

Acknowledgment—We thank A. Nakanishi for technical assistance.

REFERENCES

1. Forgac, M. (2007) Vacuolar ATPases: rotary proton pumps in physiology and pathophysiology. *Nat. Rev. Mol. Cell Biol.* **8,** 917–929
2. Yokoyama, K., and Imamura, H. (2005) Rotation, structure, and classification of prokaryotic V-ATPase. *J. Bioenerg. Biomembr.* **37,** 405–410
3. Nakano, M., Imamura, H., Toei, M., Tamakoshi, M., Yoshida, M., and Yokoyama, K. (2008) ATP hydrolysis and synthesis of a rotary motor V-ATPase from *Thermus thermophilus*. *J. Biol. Chem.* **283,** 20789–20896
4. Imamura, H., Nakano, M., Noji, H., Muneyuki, E., Ohkuma, S., Yoshida, M., and Yokoyama, K. (2003) Evidence for rotation of V_1-ATPase. *Proc. Natl. Acad. Sci. U.S.A.* **100,** 2312–2315
5. Yokoyama, K., Oshima, T., and Yoshida, M. (1990) *Thermus thermophilus*

membrane-associated ATPase: indication of a eubacterial V-type ATPase. *J. Biol. Chem.* **265,** 21946–21950
6. Tsutsumi, S., Denda, K., Yokoyama, K., Oshima, T., Date, T., and Yoshida, M. (1991) Molecular cloning of genes encoding major two subunits of a eubacterial V-type ATPase from *Thermus thermophilus*. *Biochim. Biophys. Acta* **1098,** 13–20
7. Yokoyama, K., Muneyuki, E., Amano, T., Mizutani, S., Yoshida, M., Ishida, M., and Ohkuma, S. (1998) V-ATPase of *Thermus thermophilus* is inactivated during ATP hydrolysis but can synthesize ATP. *J. Biol. Chem.* **273,** 20504–20510
8. Kakinuma, Y., Yamato, I., and Murata, T. (1999) Structure and function of vacuolar Na^+-translocating ATPase in *Enterococcus hirae*. *J. Bioenerg. Biomembr.* **31,** 7–14
9. Yokoyama, K., Nagata, K., Imamura, H., Ohkuma, S., Yoshida, M., and Tamakoshi, M. (2003) Subunit arrangement in V-ATPase from *Thermus thermophilus*. *J. Biol. Chem.* **278,** 42686–42691
10. Furuike, S., Nakano, M., Adachi, K., Noji, H., Kinosita, K. Jr., and Yokoyama, K. (2011) Resolving stepping rotation in *Thermus thermophilus* H^+-ATPase/synthase with an essentially drag-free probe. *Nat. Commun.* **2,** 233
11. Lau, W. C., and Rubinstein, J. L. (2012) Subnanometer-resolution structure of the intact *Thermus thermophilus* H^+-driven ATP synthase. *Nature* **481,** 214–218
12. Numoto, N., Hasegawa, Y., Takeda, K., and Miki, K. (2009) Intersubunit interaction and quaternary rearrangement defined by the central stalk of prokaryotic V_1-ATPase. *EMBO Rep.* **10,** 1228–1234
13. Imamura, H., Ikeda, C., Yoshida, M., and Yokoyama, K. (2004) The F subunit of *Thermus thermophilus* V_1-ATPase promotes ATPase activity but is not necessary for rotation. *J. Biol. Chem.* **279,** 18085–18090
14. Parra, K. J., and Kane, P. M. (1998) Reversible association between the V_1 and V_0 domains of yeast vacuolar H^+-ATPase is an unconventional glucose-induced effect. *Mol. Cell. Biol.* **18,** 7064–7074
15. Puopolo, K., and Forgac, M. (1990) Functional reassembly of the coated vesicle proton pump. *J. Biol. Chem.* **265,** 14836–14841
16. Parra, K. J., and Kane, P. M. (1996) Wild-type and mutant vacuolar membranes support pH-dependent reassembly of the yeast vacuolar H^+-ATPase *in vitro*. *J. Biol. Chem.* **271,** 19592–19598
17. Wilkens, S., Vasilyeva, E., and Forgac, M. (1999) Structure of the vacuolar ATPase by electron microscopy. *J. Biol. Chem.* **274,** 31804–31810
18. Iwata, M., Imamura, H., Stambouli, E., Ikeda, C., Tamakoshi, M., Nagata, K., Makyio, H., Hankamer, B., Barber, J., Yoshida, M., Yokoyama, K., and Iwata, S. (2004) Crystal structure of a central stalk subunit C and reversible association/dissociation of vacuole-type ATPase. *Proc. Natl. Acad. Sci. U.S.A.* **101,** 59–64
19. Lee, L. K., Stewart, A. G., Donohoe, M., Bernal, R. A., and Stock, D. (2010) The structure of the peripheral stalk of *Thermus thermophilus* H^+-ATPase/synthase. *Nat. Struct. Mol. Biol.* **17,** 373–378
20. Tamakoshi, M., Uchida, M., Tanabe, K., Fukuyama, S., Yamagishi, A., and Oshima, T. (1997) A new *Thermus-Escherichia coli* shuttle integration vector system. *J. Bacteriol.* **179,** 4811–4814
21. Yokoyama, K., Ohkuma, S., Taguchi, H., Yasunaga, T., Wakabayashi, T., and Yoshida, M. (2000) V-type H^+-ATPase/synthase from a thermophilic eubacterium, *Thermus thermophilus*: subunit structure and operon. *J. Biol. Chem.* **275,** 13955–13961
22. Ueno, H., Suzuki, T., Kinosita, K. Jr., and Yoshida, M. (2005) ATP-driven stepwise rotation of F_oF_1-ATP synthase. *Proc. Natl. Acad. Sci. U.S.A.* **102,** 1333–1338
23. Imamura, H., Funamoto, S., Yoshida, M., and Yokoyama, K. (2006) Reconstitution *in vitro* of V_1 complex of *Thermus thermophilus* V-ATPase revealed that ATP binding to the A subunit is crucial for V_1 formation. *J. Biol. Chem.* **281,** 38582–38591
24. Makyio, H., Iino, R., Ikeda, C., Imamura, H., Tamakoshi, M., Iwata, M., Stock, D., Bernal, R. A., Carpenter, E. P., Yoshida, M., Yokoyama, K., and Iwata, S. (2005) Structure of a central stalk subunit F of prokaryotic V-type ATPase/synthase from *Thermus thermophilus*. *EMBO J.* **24,** 3974–3983
25. Imamura, H., Nhat, K. P., Togawa, H., Saito, K., Iino, R., Kato-Yamada, Y., Nagai, T., and Noji, H. (2009) Visualization of ATP levels inside single living cells with fluorescence resonance energy transfer-based genetically encoded indicators. *Proc. Natl. Acad. Sci. U.S.A.* **106,** 15651–15656
26. Miyawaki, A., Llopis, J., Heim, R., McCaffery, J. M., Adams, J. A., Ikura, M., and Tsien, R. Y. (1997) Fluorescent indicators for Ca^{2+} based on green fluorescent proteins and calmodulin. *Nature* **388,** 882–887
27. Kitagawa, N., Mazon, H., Heck, A. J., and Wilkens, S. (2008) Stoichiometry of the peripheral stalk subunits E and G of yeast V_1-ATPase determined by mass spectrometry. *J. Biol. Chem.* **283,** 3329–3337
28. Wilkens, S., and Capaldi, R. A. (1998) ATP synthase's second stalk comes into focus. *Nature* **393,** 29
29. Stock, D., Leslie, A. G., and Walker, J. E. (1999) Molecular architecture of the rotary motor in ATP synthase. *Science* **286,** 1700–1705
30. Toei, M., Gerle, C., Nakano, M., Tani, K., Gyobu, N., Tamakoshi, M., Sone, N., Yoshida, M., Fujiyoshi, Y., Mitsuoka, K., and Yokoyama, K. (2007) Dodecamer rotor ring defines H^+/ATP ratio for ATP synthesis of prokaryotic V-ATPase from *Thermus thermophilus*. *Proc. Natl. Acad. Sci. U.S.A.* **104,** 20256–20261